

## Evaluation of NCAR Ice Nucleus Counter. Part I: Basic Operation

G. LANGER

*National Center for Atmospheric Research,<sup>1</sup> Boulder, Colo. 80302*

(Manuscript received 26 March 1973, in revised form 17 May 1973)

### ABSTRACT

A detailed examination was made of the variables affecting the operation of the National Center for Atmospheric Research (NCAR) ice nucleus counter. The design criteria for proper flow control to achieve consistent cloud formation were established. The loss of ice crystals by settling to the bottom of the cloud chamber instead of exiting to the ice crystal counter was found to be constant. The most important variable is the concentration of the cloud condensation nuclei added to the sample stream to control cloud supersaturation. The rate of activation for AgI can be increased considerably by increasing the supersaturation by the new method of combining the AgI particles with NaCl particles serving as low supersaturation condensation centers. This also gives a much faster nucleation rate of potential importance in cloud seeding. The response of kaolin and phloroglucinol under varying supersaturation was found to be in agreement with previous studies, the former being responsive to high and the latter to low supersaturation for activation. The counter provided normal temperature spectra for AgI and compared well to the Colorado State University (CSU) isothermal chamber.

### 1. Introduction

The NCAR ice nucleus counter (Langer *et al.*, 1967) is a continuous and automatically operating instrument. The distinguishing feature of the NCAR counter is the continuously operating cloud chamber which provides a controlled cloud to model natural conditions. This paper concerns itself with basic aspects of the continuous cloud chamber operation which are of general interest. The variables of concern are the humidification and cooling of the sample stream, formation of the cloud and of ice crystals, flow patterns in the chamber, and ice crystal detection. Results of a comparison against the Colorado State University isothermal chamber are included. Part II of this study will cover the reproducibility of results obtained with the NCAR counter and its comparison to the membrane filter method and the Bigg-Warner expansion chamber, using different types of nuclei.

### 2. Improved NCAR counter design and evaluation of its subsystems

#### a. Overall operation

Fig. 1 is a schematic diagram of the nucleus counter currently used by NCAR. It is based on the commercial model by EG&G<sup>2</sup> but incorporates improvements suggested by its field use in various situations. A publica-

tion describing the updating of the commercial models is in preparation. (A new model has been developed by NCAR's Facilities Laboratory but awaits evaluation in the field. Blueprints, electronic diagrams, and a manual are available from NCAR.)

In brief, the counter operates as follows: The incoming air is humidified to about 80% relative humidity at 22°C. A side stream of cloud condensation nuclei (CCN), the concentration of which can be varied, is added to the sample to control cloud density and supersaturation. The air now enters the uncooled top section of the cloud chamber and mixes with cooler air from below. This allows for more gradual cooling of the air. The chamber itself is Freon-cooled and lined with a felt of dense polyurethane foam plastic through which glycol for defrosting slowly flows to the bottom. The glycol is precooled to give a more uniform wall temperature. As the air gradually cools, ice nuclei activate the formation of ice crystals which then grow large enough to be detected by an acoustic sensor (Langer, 1972) at the exit of the chamber. The crystals can be detected by other means or collected.

#### b. Humidifier

The following problems have been encountered with past humidifier designs: humidification varied with the relative humidity of the incoming air, large dust particles passed through the humidifier and triggered the sensor, and possible nuclei losses in the humidifier were not known. Fig. 1 shows the schematic construction of the humidifier that overcomes the first

<sup>1</sup> The National Center for Atmospheric Research is sponsored by the National Science Foundation.

<sup>2</sup> First built by E. Bollay Assoc., Boulder, Colo.; then by EG&G, Boulder, Colo. (now Albuquerque, N. M.)

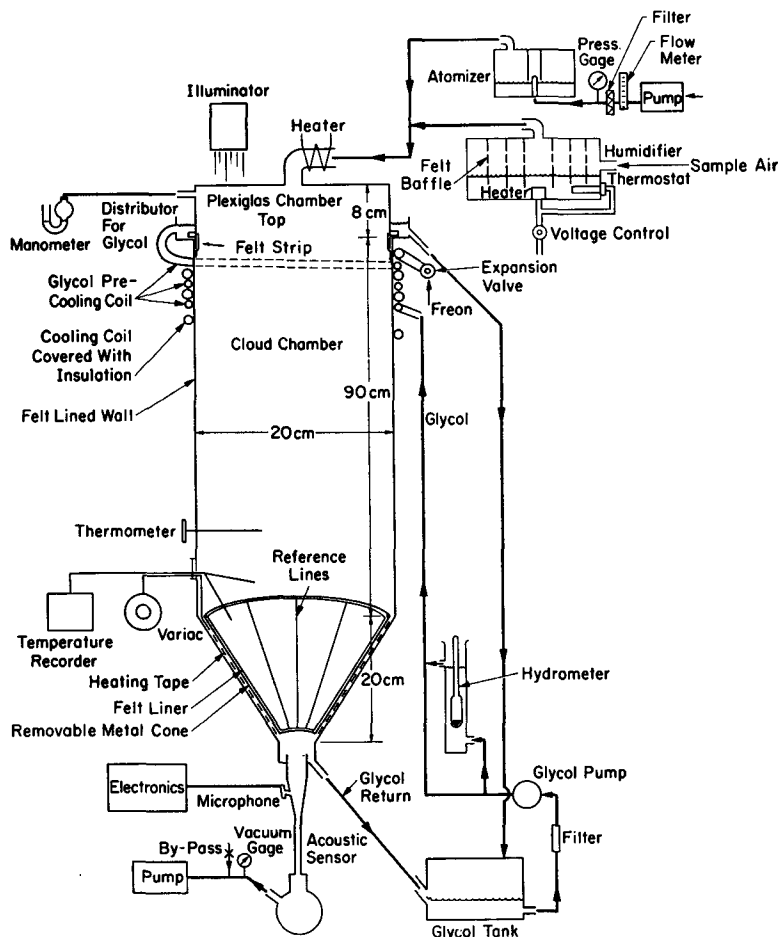


FIG. 1. Modified NCAR ice nucleus counter with removable cone insert for determining settling losses to bottom of cloud chamber.

two problems (detailed drawings are available from NCAR). A thermostat keeps the water temperature constant within  $\pm 1\text{C}$ . The distilled water level is allowed to range from 3 to 8 cm from the top. The capillary action of the felt baffles provides a source of moisture for the 10 liters  $\text{min}^{-1}$  of incoming air. The air enters from the peripheral inlet at 0.8 m  $\text{sec}^{-1}$  and large dust particles ( $> 20 \mu\text{m}$  in diameter) are impacted on the facing felt surface. If not removed, these large particles would trigger the sensor. Further removal of particles is achieved by impaction as the air passes through the multiple holes in the felt at 0.8 m  $\text{sec}^{-1}$  and impinges on the facing felt. The collection efficiency for particles with a density of 1 gm  $\text{cm}^{-3}$  and a diameter of 20  $\mu\text{m}$  is 90%. Sedimentation also removes particles, and is most effective between the outer baffles where the radial flow is 0.3 cm  $\text{sec}^{-1}$ . Crossing the first baffle gap of 2 cm takes 6 sec; in this time, 20- $\mu\text{m}$  particles settle 12 cm and are lost, while 5- $\mu\text{m}$  particles settle about 1 cm and are partially lost.

A direct evaluation of particle losses in the humidifier was made to verify the above conclusions. First, the humidifier was tested at the normal flow rate with

airborne particles large enough to trigger the acoustic sensor. The air entering and leaving the humidifier was monitored simultaneously with acoustic sensors. Test particles were lint, pollen, fly ash, glass beads and nickel spheres, covering a wide range of aerodynamic settling velocities. In no case did countable particles, i.e., those 20  $\mu\text{m}$  or larger, pass through the humidifier. Next, the penetration of laboratory air particulates in the 0.5–10  $\mu\text{m}$  range was tested with a light scattering particle counter. No loss of particles in this region could be detected. For the larger particles the uncertainty was about  $\pm 10\%$  because their concentration was low. Finally, the penetration of the humidifier by 1  $\mu\text{m}$  or smaller particles was tested with a Gardner condensation nucleus counter.<sup>3</sup> Here a loss of 20% was found for laboratory air. This figure should be used with caution since it depends on the particle size distribution of the aerosol tested.

The holdup time in the humidifier is 15 sec when the water level is 8 cm from the top. Tests were made to determine if this time is adequate for proper humidifi-

<sup>3</sup> Small Particle Detector, Type CN, Gardner Assoc., Inc., Schenectady, N. Y.

TABLE 1. Atomizer performance with 0.1% NaCl solution.

Pressure, (kg cm <sup>-2</sup> )	Condensation nuclei** from G.E. counter (cm <sup>-3</sup> )	CCN (cm <sup>-3</sup> )	Electron microscopy		
			Particles (cm <sup>-3</sup> )	Diameter (μm)	Geometric standard deviation
0.05*	3×10 <sup>3</sup> –8×10 <sup>3</sup>	—	2.7×10 <sup>2</sup>	0.07	1.5
0.2	10 <sup>6</sup> –2.5×10 <sup>6</sup>	1×10 <sup>5</sup> –3.4×10 <sup>5</sup>	2.5×10 <sup>5</sup>	0.05	1.5
0.4	4.5×10 <sup>6</sup> –8.6×10 <sup>6</sup>	5×10 <sup>5</sup> –7.10×10 <sup>5</sup>	—	—	—

\* Lowest practical setting.

\*\* Includes Aitken nuclei from filtered compressed air.

cation. An electrolytic sensing element<sup>4</sup> was used to monitor the relative humidity (RH) of the air entering and leaving. The water temperature was 22C and the air 25C. With the RH of the inlet air varying from 5 to 80%, the outlet humidity remained near 80%.

The air leaving the humidifier is combined with 1–3 liters min<sup>-1</sup> of atomizer air depending on the droplet concentration desired. This stream has a RH of almost 90%. The atomizer solution is cooled 6C due to evaporative and adiabatic cooling of the expanding air. The line heater serves to keep the combined stream from cooling if the room is cold and prevents any haze droplets from forming in the transfer line.

### c. Atomizer

The cloud condensation nucleus atomizer located as shown in Fig. 1 is constructed only of plastic material (detailed drawings are available from NCAR). Any metal parts tend to give corrosion products leading to nozzle clogging and possible production of ice nuclei. The air direction through the nozzle must be well filtered and maintained at a pressure of 0.2 kg cm<sup>-2</sup> (3 psi) if a dense cloud is desired. The device has a very strong scrubbing action for the droplets formed at the nozzle, because they must pass through myriads of air bubbles before reaching the outlet; all droplets larger than a few microns are thus removed. The remaining drops evaporate before leaving the atomizer and leave a residue of submicron salt crystals from the 0.1% NaCl solution. Electron microscope examination of the salt aerosol gave the data shown in Table 1.

The outputs of five different atomizers were tested with a General Electric condensation nucleus counter.<sup>5</sup> Table 1 summarizes the results. The CCN count was obtained with a counter being developed by NCAR (Langer, 1971a). The concentration is given as it issues from the atomizer; it is diluted four- to sixfold by the sample stream. The atomizer output also contains Aitken nuclei from the compressed air as shown by operating the atomizer dry. How many of these are lost by the scrubbing action is not known.

The activity of the salt nuclei was determined for

<sup>4</sup>Type PCRC-11 Humidity Transducer, Phys. Chem. Res. Corp., New York, N. Y.

<sup>5</sup>Model 112L428G1, Condensation Nucleus Counter, General Electric Co., Schenectady, N. Y.

the relative humidity at which they form haze droplets and the supersaturation at which the drops continue to grow. This was done with the NCAR membrane developing unit, an improved model of the device reported previously by Langer (1971b). The advantage of this device is that the tests can be run at below freezing temperatures. Formation of haze (i.e., transition to a solution drop) was noted at a saturation of 88% on a highly polished Ni-Cr foil on which the salt particles were collected with a low pressure impactor, and drops began to grow at 99% saturation with respect to water, confirming that the atomizer produces very active cloud nuclei. Activity was unaffected by temperature as reported by Roussel (1968) who showed the transition to a solution drop to be at 78% at -20C using a rather different technique and much larger crystals.

### d. Entrance flow control system and cloud characteristics

Fig. 1 shows the schematic configuration of the uncooled chamber top section which is a critical part of the cloud chamber system. The incoming air is kept at about 22C by heating the inlet line if necessary. The flow rate must be 12–14 liters min<sup>-1</sup> for proper cloud formation and acoustic sensor operation. Furthermore, the velocity of the inlet air stream is critical. If it is too fast, a warm air stream flows down the center of the chamber and some of the sample never acquires the final temperature; if it is too slow, a temperature inversion forms near the top and the air flows principally down the wall by convective cooling. This is undesirable, because the nearness of the wall causes the cloud to be dehydrated by the glycol and the flow in the central portion of the chamber becomes stagnant. Grant (1967) has reported on this flow condition.

The optimum inlet nozzle diameter was found to be 1.2–2 cm, giving a 1.2 m sec<sup>-1</sup> entrance velocity for the 1.2-cm inlet. This velocity resulted in well-defined turbulence throughout the chamber and no marked deterioration in the cloud density from top to bottom. The cloud has a dense, whitish appearance and does not turn to a bluish haze near the bottom. At higher altitudes the inlet velocity control is more important and requires the smaller nozzle.

The uncooled top section serves two purposes. First, during long-term operation it will not let the lid cool

enough to cause condensation which could lead to drops falling into the sensor. Second, it cools the air less rapidly to avoid excess supersaturation which is most likely to develop when the cloud first forms.

The inlet air stream conforms to Amelin's (1967) model of a free jet issuing into a stationary, colder gaseous medium. This leads to controlled formation of supersaturated vapor and fog by turbulent mixing. The Reynolds number is about 100 in the nozzle; this gives turbulent flow a short distance from the discharge (Schlichting, 1960). Molecular diffusion and heat conduction will then be small compared with eddy mixing. As the jet emerges from the nozzle it creates a relative vacuum; the static gas is drawn into the jet and mixed in, thus cooling the incoming air. The NaCl particles in the air become haze droplets below water saturation, and at a supersaturation of less than 0.2% these haze droplets grow to water droplets. Examination of the free jet at the top of the cloud chamber with a light beam showed a droplet-free region extending as a 4-cm long cone from the nozzle end. This cone also approximates the central aerodynamic cone which still possesses the parameters of the entering gas stream. The dimension of the aerodynamic cone was determined by probing the velocity profile with a thermo-anemometer. The fact that the aerodynamic and droplet-free cones coincide indicates that droplets form the moment the incoming air begins to mix with the cooler air. This implies that the supersaturation reached at this point is low when the atomizer provides a high concentration of CCN.

To gain a better understanding of conditions in the mixing jet and beyond, it was necessary to know the droplet concentration. This concentration was derived both by direct measurement and by calculations based on the size and concentration of the NaCl nuclei which had been determined in the atomizer performance tests. For the latter we know that at high output the atomizer produces  $10^5$  NaCl particles  $\text{cm}^{-3}$  over  $0.05 \mu\text{m}$  in diameter. These particles require only a low supersaturation to form droplets as shown in our laboratory tests (Section 2c). This aerosol is added to the sample stream and diluted about three times to give an estimated concentration of  $3 \times 10^4$  droplets  $\text{cm}^{-3}$ .

Direct measurements of concentration were accomplished by photographing the droplets as they left the bottom of the cloud chamber in an aerodynamically-defined free jet. The jet, formed by forcing air through the chamber, was rectangular in shape (1 mm deep, 2.5 cm wide, and 3 cm long) before it began to break up. The droplets were photographed in forward-scattered light from a strobe flash. A typical photo is shown in Fig. 2. The large particles in the lower photo are distorted ice crystal images. The droplet concentration was calculated to be  $8 \times 10^4 \text{ cm}^{-3}$ ; this result is in good agreement with the above calculations and justifies the use of the salt nucleus concentration as an estimate of the droplet concentration. The size range

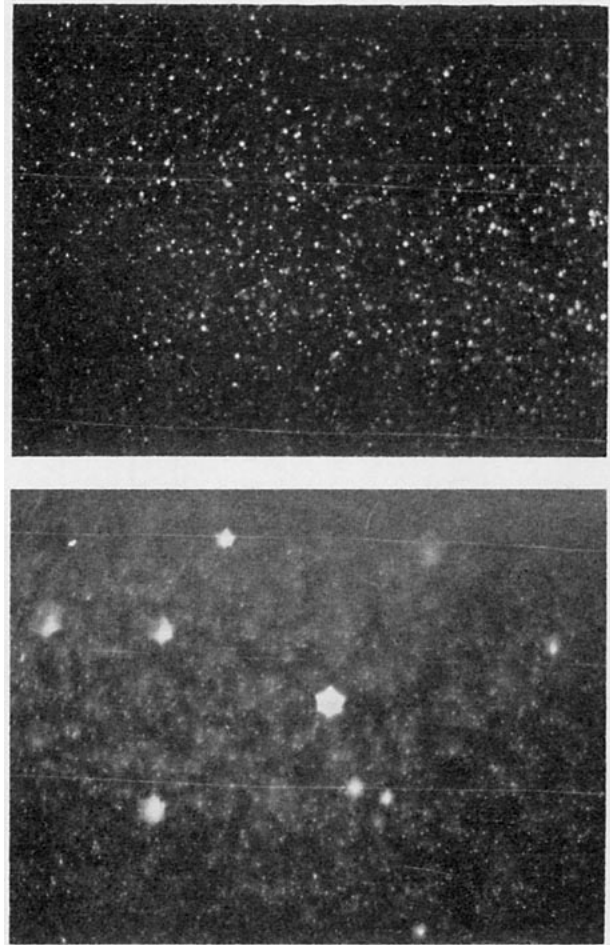


FIG. 2. Strobe flash photographs of droplets in cloud chamber: top, droplets only; bottom, droplets and ice crystals. Star shapes of crystals are due to optical distortion.

is roughly from  $1\text{--}10 \mu\text{m}$  diameter with a median of  $3 \mu\text{m}$  and a standard deviation of 1.4. The larger droplets were separately measured with a moving slide impactor and dye-coated slides. No droplets over  $12 \mu\text{m}$  in diameter were found. The liquid water content calculated from these data is about  $2 \text{ gm m}^{-3}$ , close to the measured value as described below.

Operation with a low concentration of NaCl particles is also of interest. Experimentally it was found that if the atomizer, after dilution with relatively clean sample air, provided less than  $300 \text{ CCN cm}^{-3}$  or  $300$  droplets  $\text{cm}^{-3}$ , droplets over  $20\text{--}30 \mu\text{m}$  would form and trigger the acoustic sensor. This is indicative of continued growth of the droplets after they have formed in the free jet entering the chamber. That is, as the air cools a fair amount of additional vapor becomes available for droplet growth because loss to the chamber wall is not sufficient to maintain a supersaturation below about 1–2%. By the same reasoning, the supersaturation in the free jet is still higher. To be noted is that under these conditions condensation will take place on nonsoluble particles unless they are quite small,

TABLE 2. Liquid water balance in cloud chamber.

Glycol specific gravity* (gm cm <sup>-3</sup> )	Chamber temperature (°C)	Humidifier temperature (°C)	Liquid water (gm m <sup>-3</sup> )			
			At chamber inlet**		At chamber outlet**	
			Atomizer on†	Atomizer off	Atomizer on	Atomizer off
1.09	+24	22	16.0	14.7		
1.09	+24	26	16.2		9.8	
1.08	-20	22	16.0		1.3	<1
1.08	-20	26	16.3		1.8	
1.07	+25	22	14.7		15.5	
1.07	-20	22	14.7		2.5	
1.07	-20	18	15.0		1.9	
1.07	-20	27	16.5		2.3	<1

\* At 22C.

\*\* Total flow 14.5 liters min<sup>-1</sup>, using dry, compressed air to push the air through the chamber.† 2.4 liters min<sup>-1</sup> at 0.3 kg cm<sup>-2</sup>.

i.e., <0.05 μm diameter. Tests with AgI, discussed in Section 3c, confirm these conclusions indirectly.

Humidity conditions in the cloud chamber were also inferred from direct measurements of related parameters. A PCRC electrolytic humidity sensor measured the humidity of the air exiting from the cloud chamber after the air had warmed to 10C to let all drops evaporate. This measurement was compared with the RH of the air entering the chamber; Table 2 gives the results. A substantial portion of the water vapor, about 12 gm hr<sup>-1</sup>, is taken up by the glycol. Measurement of the change in glycol level in the receiving tank yields an equal value of extracted water. A rather interesting additional observation is that when no CCN are provided and the air sample is filtered so that no cloud forms in the chamber, the liquid water content of the exit air drops markedly and is too low to support ice crystal growth in the lower part of the chamber. This would be reasonably expected since, with no drop formation, the water vapor will be absorbed more rapidly by the glycol, because no phase change is necessary, i.e., no evaporation of drops is necessary.

Despite its hygroscopic nature and its consequent complicating of the cloud conditions in the chamber, glycol is the most convenient defrosting medium. Cupric chloride and silicone oil produced much better cloud conditions but proved to be extremely difficult

to handle. The CuCl<sub>2</sub> solution attacked metallic parts of the chamber, while the silicone oil crept all over the machine and developed a tenacious ice slush. Search for a better defrosting medium merits further study.

Results reported by Auer and Veal (1968) show that the liquid water content of the cloud in their NCAR counter was much lower along with the droplet concentration. Their counter was not equipped with an atomizer and an effective humidifier. Without an atomizer the liquid water content drops as indicated in Table 2; without a good humidifier the incoming air will also be drier.

#### e. Temperature control in cloud chamber

Fig. 3 shows the temperature distribution in the chamber and illustrates the deleterious effect of not using a glycol precooling system. In most older chambers the glycol flow varies considerably along the chamber periphery because of irregularities in the header and felt lining. Where there is excess flow of glycol, cooling to the temperature of the wall is slow. This gives rise to warm areas on the wall and the resulting temperature profile variations can be seen in Fig. 3. Also, a poor cloud may form by excessive water absorption by the glycol. The ice nucleus count is reduced by the warmer temperature and poor cloud. The correction is to precool the glycol to about -10C by passing it through several feet of copper tubing into the header on top of the chamber, as shown in Fig. 1, and the final air temperature is reached at the chamber's midpoint. There is an approximate ½C temperature increase from the wall to the center in this part of the chamber. This temperature profile remains quite steady and has been verified from sea level to 3400 m. Most chambers have a variation in final temperature of ±½C over a 10-40 min period.

#### f. Cloud chamber flow of crystals and their loss in exit section

The principal question in evaluating the flow pattern of the ice crystals was to determine whether

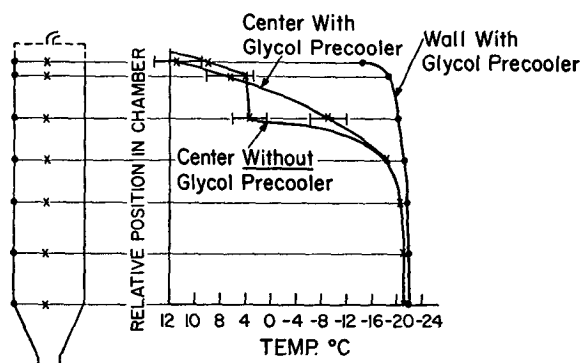


FIG. 3. Temperature profile in cloud chamber with airflow on.

crystals are lost to the bottom of the chamber and whether the residence time is long enough to let all crystals grow large enough to trigger the acoustic sensor. Since some chambers have an elbow-bend connected to a horizontal sensor to reduce the overall height, it is necessary to know whether any crystals are lost at the bend. All these factors may depend on altitude and types of nuclei as well.

To investigate these questions, a removable, conical metal liner was installed into the cone at the bottom of the chamber, as shown in Fig. 1. The cone was lined inside with plastic felt and could be heated externally with a thin, electric heating tape. The felt liner held a gel-type sugar solution (Langer and Weickmann, 1972b) which, when supercooled below  $-10^{\circ}\text{C}$ , developed visible white spots whenever ice crystals fell on it. The solution consisted of 5.6 parts commercial sweetening syrup (Karo) and 4.4 parts gelatin, with 10 drops of wetting agent added per  $100\text{ cm}^3$ . Application of the gel to the cone was a fairly complex procedure and will be described in the above publication. The tests were begun with clean air to let the gel cool to its activation temperature in the absence of nuclei. The sample was then introduced and was followed by clean air to prevent the count from becoming excessive. Fig. 4 shows the cone after exposure to ice crystals. The crystals were counted by visual inspection from above and the ice was then melted for the next use. One application of gel lasted up to 4 hr. The system was analogous to a mixing chamber with a pan of sugar solution on the bottom, except that there is a hole in the bottom to maintain continuous flow, which is not the case for an ordinary mixing chamber which works on a batchwise basis. The number of ice crystals flowing out the bottom were measured with the acoustic sensor. Comparison of this count with the number of crystals found on the cone showed that the settling loss is uniform regardless of altitude and that the modified counter has no erratic flow patterns.

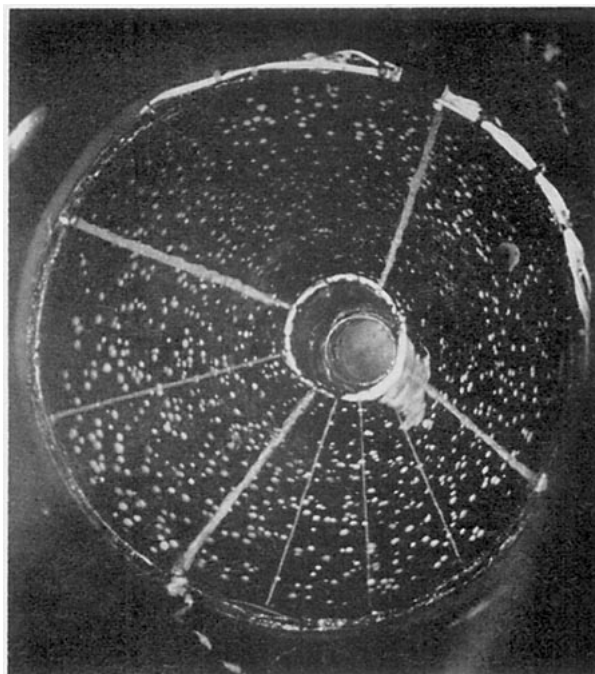


FIG. 4. Ice crystal deposit on cone insert indicating crystals lost by settling.

Table 3 summarizes data from 227 tests with AgI, phloroglucinol, kaolin, and atmospheric nuclei. The correction factor is used to multiply the acoustic sensor count to give the actual nucleus concentration. Losses result from crystals settling onto the exit cone or in the elbow and from missed counts. It is interesting to note that there is no altitude effect to at least 3300 m. For a particular test material the correction factor varied only slightly with temperature over the range of the tests ( $-10$  to  $-20^{\circ}\text{C}$ ), except for the higher temperature AgI tests discussed below. No tests are reported with the elbow in place for temperatures above  $-12^{\circ}\text{C}$  since the crystals would melt before reaching the capillary because of warming by the

TABLE 3. Correction factors for cone and elbow settling loss and missed counts.

Temperature ( $^{\circ}\text{C}$ )	Elevation (m)	Type of nuclei							
		Silver iodide		Phloroglucinol		Kaolin		Atmospheric	
		Elbow in	Elbow out	Elbow in	Elbow out	Elbow in	Elbow out	Elbow in	Elbow out
-18	30								
-9.3	1800	10	74	10		14			
-9.6	1800		41						
-10.0	1800		15						
-10.2	1800		10						
-11	1800		9		8		13		
-12	1800	11							
-13	1800			9					
-14	1800	9							
-15	1800	9		9		16			
-18	1800	10	8	10	7	12	8		9
-22	1800	10		11		15	7	14	9
-15	3300	10				14			
-20	3300	10		11	9	13	12	13	

environment. For a particular test series the variation in correction factors was no more than  $\pm 10\%$ .

Differing correction factors for various chemicals were expected. Phloroglucinol and AgI act promptly, and since their final (lowest) temperature was reached about halfway down the chamber (see Fig. 3) the crystals all had time to grow to over  $20\ \mu\text{m}$  diameter once they were activated at their temperature threshold. In this case no missed counts were encountered. By contrast, slower acting particles such as kaolin and atmospheric nuclei were activated continuously as they flowed through the lower half of the chamber and a fraction of the crystals produced were too small to trigger the acoustic sensor. This resulted in the higher correction factors. At higher temperatures where AgI also acts more slowly, the effect is similar. As shown by the data for the range between  $-9.2$  and  $-10.2^\circ\text{C}$  this effect becomes rather pronounced.

Our correction factors for the loss of crystals nucleated by AgI disagree with those of Middleton and Auer (1970) who collected a sample of ice crystals on a microscope slide inserted through the observation window near the bottom of the chamber. Their results showed that the acoustic sensor missed only half the crystals. However, the collection efficiency of the slide was not established. Some crystals will drift around the slide. Our results were obtained over a period of one-half year at four locations with four modified counters. The results were quite consistent. Different cone angles, including a much steeper angle, were tried to reduce the settling losses, but no changes occurred; and the present  $60^\circ$  angle design was found best from an operational standpoint.

#### *g. Counting of ice crystals*

Some details regarding the operations of the acoustical sensor are in order. Areas of interest are echo counts, sensor temperature, contamination, microphone attachment, electronic noise, and altitude effect on the signal.

The audible click (Langer, 1972) generated by an ice crystal flowing through the sensor travels as a sound wave into the chamber and bounces principally off the flat plexiglass chamber lid. If the echo is strong enough it will trigger the counting circuit a second time 7 msec later and possibly even a third time. An enlarged lid lined with fiberglass completely suppresses the echo; a lining of crinkled household aluminum foil suppresses the echo considerably. However, these modifications limit the view of the chamber walls and the cloud. Usually one compromises by setting the time delay of the counting circuit to about 8 msec to eliminate the first echo.

Exhaust pump air is passed over the sensor to keep its temperature above that of the chamber in order to avoid internal condensation. This precaution prevents the formation of drops that can roll along the wall into the capillary and produce a rustling or screeching noise giving extra counts. However, if too much heat

is applied the ice crystals may start to evaporate or even melt. Another source of spurious signals is the accumulation of dust deposits in the contracting section of the sensor and the capillary during several weeks of operation. The deposits produce noise by presenting a rough wall surface (Langer, 1969).

The microphone must be attached tightly to avoid air leaks and the microphone vent must be glued shut. The use of a sound-transmitting plastic film to seal the sensor from the microphone is not recommended. The sound transmission of the film varies with its tension.

Electronic noises have been a problem, especially in long-term unattended operation, which is often in remote areas where voltage, frequency regulation and grounding may be inadequate. An isolation transformer will often filter out line spikes but each location may nevertheless have its own problems. Periodic checks should be made with all components operating but with the microphone disconnected from the sensor. Any counts recorded are due to electronic and possibly mechanical noise.

Increasing altitude weakens the signal strength until above 4600 m the signal is near the noise level. At the same altitude the flow of crystals in the chamber changes to a relatively straight-line path and the loss to the bottom cone increases drastically. Pressurized operation of the counter is feasible, as demonstrated with the NCAR cloud condensation nucleus counter (Langer, 1971a) which is based on a similar principle.

### **3. Study of the nucleation processes in the NCAR counter**

#### *a. Comparison of the NCAR counter vs the CSU isothermal chamber*

Steel *et al.* (1967) first calibrated an NCAR counter against the CSU isothermal chamber (Steele and Krebs, 1967). The chamber simulates natural conditions closely and is the standard for calibrating AgI seeding generators and flares. Steele *et al.* found that the CSU chamber counted three times more nuclei than the NCAR counter. The CSU chamber has been improved considerably in the intervening years and probably achieved its optimum configuration in mid-1971. In May 1972 an aircraft type NCAR counter was compared again during the calibration of a Montana State University modified Skyfire generator using AgI-NH<sub>4</sub>I (Colorado State University, 1972). The counter had a top section that is not raised as in Fig. 1 but is flush with the cooled part of the cloud chamber. This results in more rapid cooling of the incoming air and gives a higher supersaturation. The two NCAR counter models were compared with AgI nuclei and the aircraft unit gave twice the count with the same atomizer setting.

The NCAR counter sampled continuously from the wind tunnel. The tunnel provides a controlled combus-

tion environment and dilutes the generator output. Since the concentration in the tunnel was still too high for direct sampling by the NCAR counter, a special diluter was used to dilute the smoke by a factor of  $2 \times 10^6$ . The CSU cloud chamber receives a syringe sample from the wind tunnel that is diluted before injection.

The two systems agreed well using the correction factor with the elbow in for the NCAR counter given in Table 3. At  $-20^\circ\text{C}$  the NCAR counter with the  $0.2 \text{ kg cm}^{-2}$  atomizer setting gave  $1.7 \times 10^{15}$  nuclei per gram of AgI while the CSU chamber gave  $8.5 \times 10^{14}$  nuclei  $\text{gm}^{-1}$ . Data on the AgI aerosol concentration measured in the wind tunnel versus the nucleus counts give further useful information. Undiluted smoke was sampled directly from the tunnel with an electrostatic precipitator<sup>6</sup> but without a charge neutralizer. A correction factor of 10 was estimated for the charged aerosol particles that precipitated out before the sampling area; the factor was based on the density of the particle deposition. A concentration of  $3.5 \times 10^{11}$  particles  $\text{liter}^{-1}$  was found for the CSU wind tunnel vs  $7.5 \times 10^9$  nuclei  $\text{liter}^{-1}$  from the NCAR counter for the wind tunnel concentration. Thus, about 2% of the particles were nucleated at  $-20^\circ\text{C}$ . The particle size ranged from 0.01 to  $0.07 \mu\text{m}$ , with a median diameter of  $0.03 \mu\text{m}$ . Many of the small particles would not be expected to nucleate. No evidence of combustion particles was noted in shadowed electron microscope samples (Fig. 5).

No effort was made to ascertain the effect of cloud droplet concentration on the NCAR counter counts. Both cloud chambers operated with dense clouds. The CSU chamber utilizes an ultrasonic atomizer to provide

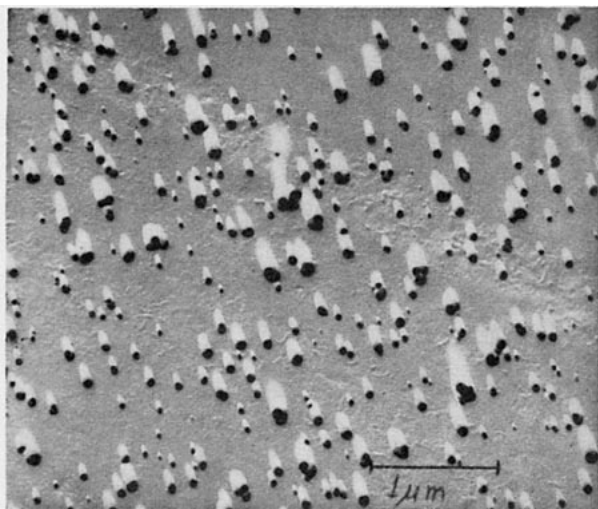


Fig. 5. Electron microscope photograph of AgI particles from a AgI-NH<sub>4</sub>I Skyfire generator used in the NCAR counter-CSU isothermal chamber comparison.

<sup>6</sup> Model 3100 Electrostatic Sampler, Thermo-Systems, Inc., St. Paul, Minn.

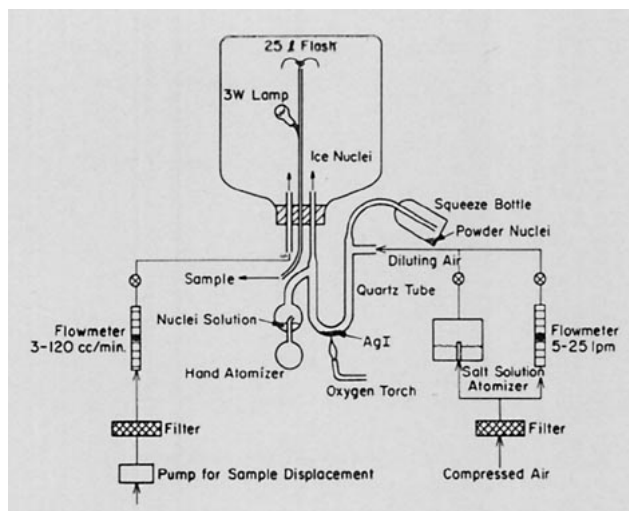


Fig. 6. Ice nucleus generating system for laboratory tests.

a cloud with a liquid water content of  $1.5 \text{ gm m}^{-3}$  and a median droplet diameter of  $5 \mu\text{m}$ . The NCAR counter had much less hold-up time but yet counted more nuclei because it operated at a higher supersaturation.

#### b. Temperature spectrum determination

The operation of the NCAR counter at different chamber temperatures is important for evaluating cloud seeding agents and natural nuclei activity. This section deals with the control of the variables involved and tests with AgI nuclei to compare against previously reported information.

The test aerosols were generated in the system shown in Fig. 6 with two NCAR counters operating in parallel to sample the supply flash. The thermally generated AgI particles are produced by momentarily heating a small deposit of chemical grade AgI to red heat in the bottom of the quartz U-tube with an oxygen torch. Filtered air passes over the AgI at  $15 \text{ liters min}^{-1}$  to quickly quench the vapors and to prevent excessive agglomeration of the particles. The result is an aerosol in the  $0.01\text{--}0.3 \mu\text{m}$  range consisting of small chain-like particles. AgI powder is dispersed from a vigorously shaken plastic squeeze bottle into the  $15 \text{ liters min}^{-1}$  air stream to give an aerosol in the  $0.3\text{--}3 \mu\text{m}$  range. The diluting air stream is quickly shut off from the powder but is left on for about 5 min for the smoke to dilute it sufficiently for counting. The 25-liter flask is emptied into the main air stream at  $3 \text{ cm}^3 \text{ min}^{-1}$  for the smoke and  $15 \text{ cm}^3 \text{ min}^{-1}$  for the powder aerosol. The counters can operate on this supply for many hours. The small pilot light in the flask maintains convection to mix the smoke. The procedure for determining the temperature spectrum is to hold one counter at  $-20^\circ\text{C}$  as a reference unit and to vary the temperature of the second unit. About one-half hour is allowed after a temperature change for the system to equilibrate. The initial drop in count upon warming the chamber

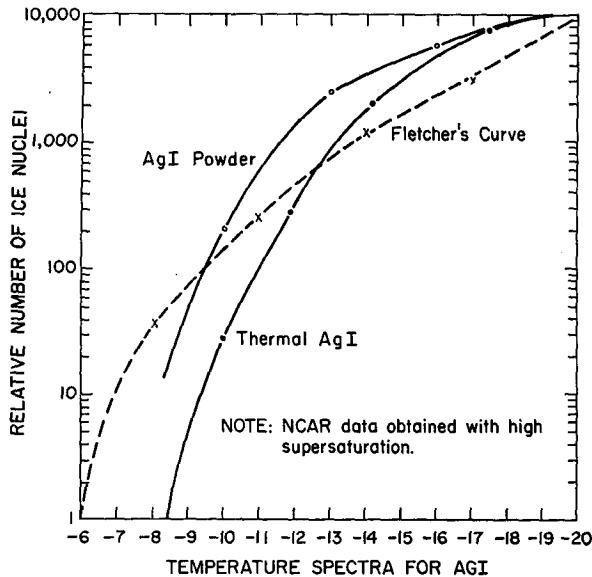


FIG. 7. Temperature spectra from NCAR counter for different AgI aerosols generated in the laboratory.

is higher than the final change. The temperature spectrum is derived from the ratio of counts between the two counters at a given time. The humidifier temperature is increased as the chamber warms to maintain a constant cloud density. For chamber temperatures of  $-20$ ,  $-15$  and  $-10^{\circ}\text{C}$ , the humidifier temperature was  $22$ ,  $30$  and  $40^{\circ}\text{C}$ , respectively.

The temperature spectrum for the AgI powder is given in Fig. 7. From  $-21$  to  $-16^{\circ}\text{C}$  the activity dropped by a factor of  $1.7$  and from  $-21$  to  $-13^{\circ}\text{C}$  by a factor of  $4.0$ . Considering the size of the particles this is a reasonable result. At  $-10^{\circ}\text{C}$  the powder shows considerably more activity than the thermally generated AgI smoke (see Fig. 7) which has much smaller particles. The agreement with the shape of the theoretical curve (from Fletcher, 1962) is as good as can be expected, since the theory is based on AgI acting as a deposition nucleus.

### c. Modes of nucleation in the NCAR Counter

Of fundamental importance is how nucleation proceeds in the counter so the results can be related to conditions found in nature. The following nucleation processes are possible: 1) A droplet and a nucleus collide and nucleate to ice immediately or after further cooling. 2) The nucleus acts initially as a condensation nucleus and a water drop forms around it or around a particle attached to it; the ice phase forms on further cooling. 3) Water vapor deposits directly onto the nucleus to form ice.

In contact nucleation the nucleus presumably resides on the droplet surface after collision, and when freezing occurs a whole drop is frozen instead of a thin water film as expected on a condensation-freezing nucleus

activated near its freezing temperature. The former results in a distinct crystal structure, i.e., a small frozen drop as a center (Parungo, 1972) and as observed in the field by Auer (1972) during AgI seeding. Other investigators also consider contact nucleation to be an important mechanism for AgI and probably for other nuclei as well (Sax and Goldsmith, 1972; Genadiev, 1972; Gokhale and Lewinter, 1971). In our cloud chamber, using a droplet concentration of  $8 \times 10^4 \text{ cm}^{-3}$  and an average interaction time of  $45 \text{ sec}$  (the nominal hold-up time in the chamber is  $90 \text{ sec}$ ), one can calculate the rate of Brownian diffusion contact, leaving aside any phoretic effects. Referring to Fuchs (1964) one finds that for nuclei of  $0.01$ ,  $0.1$  and  $1.0 \mu\text{m}$  radius,  $4$ ,  $0.1$  and  $0.004\%$  of these particles are scavenged by a  $3\text{-}\mu\text{m}$  radius water droplet in  $1 \text{ sec}$ . Except for the very small nuclei it is obvious that Brownian diffusion would not provide much droplet contact in our cloud chamber. This also holds in nature where the droplet concentration is much lower but more time is available (Slinn, 1971; Isaac, 1972). This points to poor utilization of the AgI, especially for larger particles, which have less Brownian motion. But the larger ones should be more active by deposition or condensation and at warmer temperatures (Edwards and Evans, 1960). Fletcher (1959) points out, though, that they still require a fair water supersaturation for such activity.

The balance between the possible nucleation mechanisms was examined. Fig. 8 shows the effect of droplet concentration on the count with thermally generated AgI (see Section 3b) which had particles in the  $0.01\text{--}0.3 \mu\text{m}$  range. There is an inverse relationship of count with droplet concentration. The nature of the cloud chamber system is such that the degree of supersaturation is also inversely related to the droplet concentration. This indicates that nucleation due to deposition and condensation should be enhanced by a reduction in drop concentration. This enhancement is much stronger, as seen from Fig. 8, than the response to increasing the droplet concentration to promote contact nucleation. But as pointed out above contact is a limited process. However, Middleton and Auer (1970) report that  $35\%$  of the ice crystals in an NCAR counter that they seeded with AgI had frozen droplet centers. This does not prove contact nucleation as they suggested because condensation could have taken place in the upper part of the chamber before freezing temperatures were even reached. The drops thus formed will grow to the size observed in the crystal and then freeze further down in the chamber; crystal formation then begins.

The rate of condensation versus deposition is difficult to define accurately, but above water saturation it is unlikely that deposition can proceed effectively since condensation to the liquid phase is facilitated by an increase in supersaturation and can occur before freezing temperatures. This is true in our cloud chamber where the highest supersaturation exists above freezing

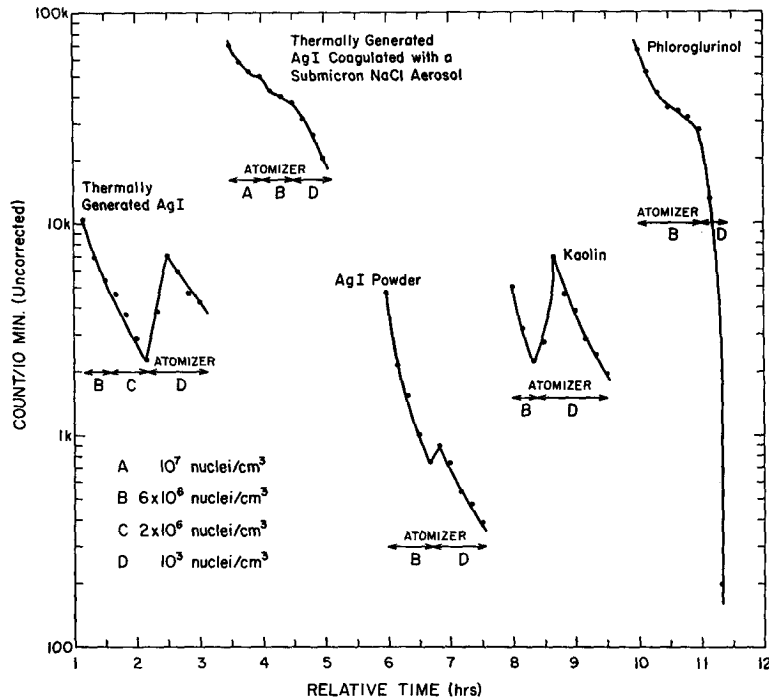


Fig. 8. Effect of atomizer pressure (supersaturation) on ice nucleus count.

temperatures in the free jet at the top as the cloud forms; thus, deposition should be unimportant. In nature the highest supersaturation also exists at warmer temperatures at cloud base.

This leaves condensation-freezing as an important process, because the rate of contact nucleation is low (Edwards and Evans, 1961; Davis and Auer, 1971) and deposition is limited. So the opportunities for condensation should be examined further. It is controlled by the supersaturation requirements, which may be reduced by contaminants or additives in the nucleant composition. Also, transient high supersaturations may exist in clouds near freezing drops at least (Rosinski *et al.*, 1971; Rosinski and Kerrigan, 1972; Nix and Fukuta, 1972). Tests were made to demonstrate the effect of additives to AgI to promote condensation at lower supersaturation. A pure AgI aerosol was coagulated with a NaCl aerosol. The rate of nucleation increased fourfold in the NCAR counter everything else being equal. Odencrantz (1968) found that AgI contaminated with some air pollutants exhibited increased activity.

Further information on condensation-freezing activity is given below for AgI and other artificial nucleants. Tests with AgI powder particles in the 0.3–3 μm range show that the droplet concentration in the NCAR counter or the related degree of supersaturation has little effect on the nucleus count (see Fig. 8). Obviously these particles have little Brownian motion and hence a low collision rate with water droplets; on the other hand, condensation takes place much more

easily on such large particles, i.e., at a 2% supersaturation for pure AgI (Fletcher, 1959). The particles all nucleate at -21C as verified by microscopic counts of the AgI aerosol concentration (Langer and Weickmann, 1972a). Kaolin responds better at lower cloud drop concentrations, indicating that it requires a higher supersaturation for condensation. These results also indicate that the nuclei are in contact with relatively warm liquid water because condensation takes place at the top of the chamber. For a short time interval this evidently does not affect the nuclei adversely. On the other hand, phloroglucinol responds best at a fairly high droplet concentration, i.e., at lower supersaturation. This indicates that if condensation is too high the particles are deactivated. Since phloroglucinol is fairly water soluble, this is not surprising.

#### 4. Conclusions

The variables affecting the operation of the NCAR ice nucleus counter have been examined. Provided that a properly constructed and operated counter is used, the most important variable is the concentration and activity of the cloud condensation nuclei (CCN) added to the sample stream. These nuclei control the supersaturation (SS) achieved during the initial cloud formation process in the entrance jet which in turn has a strong influence on the number of ice nuclei activated when the cloud is cooled. This variable is largely controlled by the salt solution atomizer that provides artificial CCN. In unusual circumstances, the air may contain a large number of CCN and full control over

the SS in the range of interest cannot be achieved. Control over the SS is exerted by varying the concentration of the CCN and by adjusting the free jet mixing process at the inlet of the chamber. The highest SS is found in the envelope of the free jet as it mixes with the surrounding cooler air. The CCN provides a sink for the water vapor by the condensation process and thus control the SS. Once the initial cloud has formed, further nucleation of CCN is unlikely because the available water surface on the cloud droplets limits the SS to a low value as additional cooling takes place. Thus, in the later phase of the cloud cooling process interaction of water with particles can be achieved only by collision with drops or deposition of vapor directly to ice. The former is again controlled by the CCN concentration. The results so far indicate that collision of nuclei with drops is not efficient timewise, as is to be expected from theoretical calculations.

It is obvious that the inlet air flow pattern is an important variable since it determines how the inlet jet mixes with the surroundings. Consequently, the inlet nozzle should give a uniform, turbulent flow velocity profile with an average velocity of about  $1.5 \text{ m sec}^{-1}$ . The inlet flow conditions also control the flow in the remainder of the chamber, which should be uniformly turbulent throughout.

It is interesting to summarize the response of different nucleus types as the CCN concentration changes under fixed conditions of humidifier temperature, and inlet nozzle configuration. For thermally generated AgI in the  $0.01\text{--}0.3 \mu\text{m}$  range, the count at  $-20\text{C}$  was reduced by a factor of 4 with a high droplet concentration ( $10^5 \text{ cm}^{-3}$ ), which gives a low SS. With a droplet concentration of only  $300 \text{ cm}^{-3}$  or a high SS the count reached a maximum because more nucleation by condensation took place. When the same AgI aerosol was mixed with a salt aerosol in the 25-liter supply flask, maximum effectiveness was found regardless of the CCN concentration; that is, the NaCl particles that were attached to the AgI particles by coagulation served as efficient condensation centers. The most important aspect of this process is that nucleation is not delayed until a relatively rare collision with a supercooled water droplet takes place. The activity of AgI powder particles from  $0.3$  to  $3 \mu\text{m}$  was also nearly independent of drop concentration. These large AgI particles act as more effective CCN.

*Acknowledgments.* Thanks are due to Joachim Weickmann, now at Colorado State University, who determined the settling losses to the bottom of the cloud chamber; to T. Cannon, NCAR, who suggested the procedure for photographing the droplets in the cloud chamber; to D. Belsher, University of Colorado, who assisted with the laboratory work; to J. Rosinski, NCAR, for many helpful discussions; and to C. Garcia, NCAR, whose conscientious operation of an NCAR counter at the Mauna Loa Observatory, Hawaii, de-

lined various problems related to the operation of the counter and contributed to their solution. This work was accomplished in partial support of the National Hail Research Experiment.

#### REFERENCES

- Amelin, A. G., 1967: *Theory of Fog Formation*. Israel Program for Scientific Translations, Jerusalem, 61–92.
- Auer, A. H., 1972: Inferences about ice nucleation from ice crystal observations. *J. Atmos. Sci.*, **29**, 311–317.
- , and D. V. Veal, 1968: Characteristics of the cloud within the NCAR ice nucleus counter. *J. Rech. Atmos.*, **3**, 155–165.
- Colorado State University, 1972: Montana State Skyfire ground generator effectiveness tests with AgI-NH<sub>3</sub> solution. Rept. 7204C, Cloud Simulation and Aerosol Laboratory, Colorado State University, 19 pp.
- Davis, C. I., and A. H. Auer, 1971: The possibility of collision nucleation by an AgI aerosol. *Preprints Intern. Conf. Weather Modification*, Canberra, Australia, Amer. Meteor. Soc., 12–16.
- Edwards, G. R., and L. F. Evans, 1960: Ice nucleation by AgI. I. Freezing vs. sublimation. *J. Meteor.*, **17**, 627–634.
- , and —, 1961: Ice nucleation by AgI. II. Collision efficiency in natural clouds. *J. Meteor.*, **18**, 760–765.
- Fletcher, N. H., 1959: On ice crystal production by aerosol particles. *J. Meteor.*, **16**, 173–180.
- , 1962: *The Physics of Rainclouds*. Cambridge University Press, p. 318.
- Fuchs, N. A., 1964: *The Mechanics of Aerosols*. New York, Pergamon Press, 194–195.
- Genadiev, N., 1972: Über die Lage der AgI-Aerosol-Gefrierkerne in Wassertropfen. *Proc. Bulgarian Acad. Sci.*, **23**, 503–506.
- Gokhale, N. R., and O. Lewinter, 1971: Microcinematographic studies of contact nucleation. *J. Appl. Meteor.*, **10**, 469–473.
- Grant, L. O., 1967: Ice nuclei and other studies of opportunity during the 1967 Yellowstone Expedition. Final Report, 7th Yellowstone Field Research Expedition, Atmospheric Science Center, New York State University, Albany, 80–88.
- Isaac, G. A., 1972: Another “time lag” in the activation of atmospheric ice nuclei. *J. Appl. Meteor.*, **11**, 490–493.
- Langer, G., 1969: Status of acoustic particle counter research. *J. Powder Tech.*, **2**, 307–308.
- , 1971a: NCAR continuous cloud condensation nucleus counter. *Second International Workshop on Condensation and Ice Nuclei*, Dept. Atmos. Sci., Colorado State University, 45–46.
- , 1971b: NCAR ice nucleus analyzer. *Second International Workshop on Condensation and Ice Nuclei*, Dept. Atmos. Sci., Colorado State University, 55–56.
- , 1972: Further evaluation of the acoustical particle counter. *J. Powder Tech.*, **6**, 5–8.
- , and J. Weickmann, 1972a: A comparison of various techniques to count AgI nuclei with emphasis on the membrane technique. *J. Rech. Atmos.*, **6**, 335–342.
- , and —, 1972b: Ice crystal loss to the bottom of the continuous cloud chamber in the NCAR ice nucleus counter. *J. Rech. Atmos.*, **6** (in press).
- , J. Rosinski and C. P. Edwards, 1967: A continuous ice nucleus counter and its application to tracking in the troposphere. *J. Appl. Meteor.*, **6**, 114–125.
- Middleton, J. R., and A. H. Auer, 1970: Ice crystal growth within the NCAR ice nucleus counter. *Preprints Conf. Cloud Physics*, Ft. Collins, Colo., Amer. Meteor. Soc., 87–88.
- Nix, N., and N. Fukuta, 1972: Nonsteady-state kinetics of droplets in cloud physics. *Abstracts Intern. Cloud Physics Conf.*, London, Roy. Meteor. Soc., 25–26.
- Odencrantz, F. H., 1968: Modification of the ice nucleation efficiency of pyrotechnically produced AgI smoke by atmospheric contamination. *J. Appl. Meteor.*, **7**, 955–956.

- Parungo, F. P., 1972: Electron-microscope study of AgI as contact or sublimation nucleus. *Preprints Third Conf. Weather Modification*, Rapid City, S. D., Amer. Meteor. Soc., 5-7.
- Rosinski, J., and T. C. Kerrigan, 1972: Mechanism of ice formation in seeded convective storms. *Z. Angew. Math. Phys.*, **23**, 278-300.
- , G. Langer, C. T. Nagamoto and T. C. Kerrigan, 1971: Natural ice-forming nuclei in severe storms. *J. Atmos. Sci.*, **28**, 391-401.
- Roussel, J. C., 1968: Determination de l'hygroscopicité critique des sels à température négative. *J. Rech. Atmos.*, **3**, 253-262.
- Sax, R. I., and P. Goldsmith, 1972: Nucleation of water drops by Brownian contact with AgI and other aerosols. *Quart. J. Roy. Meteor. Soc.*, **98**, 60-72.
- Schlichting, H., 1960: *Boundary Layer Theory*. New York, McGraw-Hill, p. 181.
- Slinn, W. G. N., 1971: Time constants for cloud seeding and tracer experiments. *J. Atmos. Sci.*, **28**, 1509-1511.
- Steele, R. L., and F. W. Krebs, 1967: Characteristics of AgI ice nuclei originating from anhydrous  $\text{NH}_3$ -AgI complexes. *I. J. Appl. Meteor.*, **6**, 105-113.
- , C. P. Edwards, L. O. Grant and G. Langer, 1967: A calibration of the NCAR acoustical ice nucleus counter. *J. Appl. Meteor.*, **6**, 1097-1107.